Aluminum–cerium double-metal impregnated activated carbon: a novel composite for fluoride removal from aqueous solution

Shreeya Kalidindi, Mounica Vecha, Arkamitra Kar and Trishikhi Raychoudhury

ABSTRACT

Several studies have focused on the application of layered double hydroxide or nanoparticle based adsorbent for removing fluoride. The objectives of this study are to impregnate aluminum (Al) and cerium (Ce) within the pore spaces of activated carbon (AC) for removal of fluoride from water and to evaluate the partitioning behavior of fluoride by the double-metal-AC composite. To achieve the objectives, combined oxides/hydroxides of Al and Ce were impregnated within the pore spaces of AC under varying pH, metal concentration, and synthesis temperature. The fluoride removal by different composite was evaluated, and the best performing composite was selected for equilibrium sorption experiments and kinetic tests. The effect of pH on fluoride removal was assessed. Overall it was observed that impregnation of a small amount of metal (0.05 mol/L Al-Ce) can enhance the fluoride removal efficiency, compared to unmodified AC. Sorption of the best performing composite follows the Freundlich isotherm model. The maximum fluoride sorption capacity was estimated as 3.05 mg F^-/g of composite. The rate of sorption by the selected composite is reasonably fast (3.6/h). Furthermore, within a wide range of pH (5–10), removal of fluoride was observed to be consistent.

Key words | composite material, equilibrium sorption, filter media, fluoride removal, kinetics

Shreeya Kalidindi
Mounica Vecha
Arkamitra Kar
Trishikhi Raychoudhury (corresponding author)
Department of Civil Engineering,
BITS-Pilani Hyderabad Campus,
Jawahar Nagar, Shameerpet Mandal, Ranga Reddy District,
Hyderabad 500078,
India
E-mail: *trishikhi@iitp.ac.in*; *trishirc@gmail.com*

Trishikhi Raychoudhury
Department of Civil and Environmental Engineering,
Indian Institute of Technology Patna,
Bihta,
Patna,
Bihar 801103,
India

INTRODUCTION

Excessive fluoride (F^-) concentration in the groundwater was identified as a potential source of health hazard in many parts of the world. Occurrences of fluoride are mostly geogenic. An acceptable limit of F^- concentration in drinking water is within the limit of 0.5–1.5 mg/L (WHO 2006). However, millions of people consume F^- contaminated drinking water daily. Fluoride intake can cause dental fluorosis, skeleton fluorosis, and long-term exposure can even affect the reproductive and neural systems (WHO 2006).

Alum is a traditionally used chemical for removing fluoride from water. Applications of different metal-based oxides for fluoride removal have been investigated extensively. Several recent studies have reported that F^- removal has improved significantly by application of layered double hydroxides (LDH) of metals (Mohapatra *et al.* 2009; Bhatnagar *et al.* 2011). Application of nanoparticles (NPs) is becoming an emerging technique for remediation of water and wastewater (Mohapatra *et al.* 2009; Bhatnagar *et al.* 2011; Miretzky & Cirelli 2011; Raychoudhury & Scheytt 2013), given the fact that they have extensively high specific surface area (SSA). The main limitation of the application of NPs for drinking water quality control is their aggregation behavior. Furthermore, there might be some risk associated with the release of NPs into the treated water. On the other hand, granular activated carbon (AC) having very high SSA and good mechanical resistance, is commonly used as filtering material for water purification. Thus, there is scope for impregnating multiple metal-based oxides/hydroxides within the pore spaces of AC, so that the high SSA of AC can be combined with adsorption active sites of metal

doi: 10.2166/ws.2016.114

oxides. The advantages of the composite are (i) aggregation of NPs can be avoided and (ii) any possible risk of releasing NPs in drinking water can be minimized.

Based on this hypothesis, several studies have explored the possibility of applying AC-metal composite for removal of arsenic from drinking water (Gu *et al.* 2005; Choi *et al.* 2008; Hristovski *et al.* 2009; Chang *et al.* 2010; Raychoudhury *et al.* 2015). However, there are limited studies on the application of AC-metal based novel composites for removal of F^- from the water. Few recent studies have explored the possibility of impregnating a single metal within the micropores of different non-metallic materials (He *et al.* 2014; Zhang *et al.* 2014; Yu *et al.* 2015). However, anchoring double metal based oxides/hydroxides within the pores of AC is not explored widely, especially for removing F^-. Furthermore, the efficiency of a composite is dependent on the synthesis conditions (Hristovski *et al.* 2009; Raychoudhury *et al.* 2015), and those conditions need to be optimized for any novel composite. The objectives of the present study are, therefore, to optimize the impregnation conditions of double-metal (Al-Ce) within the pore spaces of AC for removing fluoride, and to evaluate the partitioning behavior of fluoride from the aqueous phase to the solid surface of the composite. Liu *et al.* (2010) have demonstrated that the F^- adsorption capacity of Al-Ce hybrid metal is significantly high (68 mg/g). A trimetallic Al-Ce-Fe composite also shows promising performance for removing F^- from water (Wu *et al.* 2007). Relevant preliminary experiments for the present study (data not shown) indicate that the addition of Fe in AC-AlCe composite reduces the performance of the adsorbent. Based on this observation, Al and Ce were considered as suitable metals for synthesizing the composite material. To evaluate the optimal synthesis condition, oxides/hydroxides of aluminum and cerium were impregnated within the pore spaces of AC under varying pH, metal concentration, and synthesis temperature. The F^- removal by different composite was evaluated, and the best performing composite was selected for further study. The possibility of dissolution of impregnated metal (Al, Ce) for the best performing composite was checked. Equilibrium sorption experiments and kinetic tests were carried out, and the data were compared with available models to evaluate the sorption behavior of fluoride by the selected composite. Furthermore, the effect of pH on F^- removal efficiency was assessed.

MATERIAL AND METHODS

Material

Granular activated carbon (Darco 12–20 mesh: 850–1,000 μm size), and sodium fluoride (NaF) were obtained from Sigma-Aldrich. Reagent grade salts of different metals such as cerium nitrate [$Ce(NO_3)_3$, $6H_2O$], and aluminum sulfate [$Al_2(SO_4)_3$, 16 H_2O] were obtained from Hychem Pvt. Ltd (SDFCL). To adjust pH, reagent grade sodium hydroxide (NaOH) or hydrochloric acid (HCl) was used. Millipore de-ionized (DI) water was used for all purposes throughout the experiments.

Synthesis of AC–aluminum–cerium composites

The granular activated carbon–aluminum–cerium (AC-AlCe) composites were synthesized under a range of initial pHs (2.5–5). The optimal concentration of metal was assessed by synthesizing the composite under varying metal concentration (0.05 mol/L to 0.21 mol/L) at two different temperatures (120 °C and 240 °C), keeping the molar ratio of Al and Ce constant at 8:1.

The synthesis process was kept similar to that adopted in Raychoudhury *et al.* (2015). Granular activated carbon was washed with DI water thoroughly and dried overnight (15 h) at 105 °C to remove finer AC particles and other impurities. Then, four composites were synthesized with varying pHs keeping the concentration of metal constant at 0.09 mol/L. In our previous study (Raychoudhury *et al.* 2015), impregnation of 0.09 mol/L iron within the pore spaces of AC resulted in the maximum removal capacity of arsenic. Considering this fact, the same concentration of metal (0.09 mol/L) was taken as the initial synthesis condition for the composites. In a separate system, a number of solutions were prepared with varying concentrations of metal (ranging from 0.05 mol/L to 0.21 mol/L) by mixing Al and Ce salts, keeping the Al/Ce ratio constant at 8:1, with a fixed pH of 2.5; 250 mL of different solutions containing Al-Ce salts were poured in to a series of conical flasks, each containing 10 g of AC. In the case of varying pH, the pH of the mixture was adjusted at this point by adding 0.1 mol/L NaOH. All the mixtures were kept overnight (15 h) at room temperature to allow diffusion of metal ions or deposition of precipitate in the pore spaces of AC. After

stabilization, excess solution was discarded and rinsed with DI water to remove free metal ions or precipitates. The residual samples were treated at 120 °C temperature for 5 h or 240 °C for 2 h. After synthesis, all the composites were rinsed several times with DI water to remove excess metal ions or particulate metal oxides/hydroxides. Finally, the AC-AlCe composites were dried at 105 °C and stored air-tight. Details of the composite and their synthesis conditions are summarized in Supplementary Table S1 (available with the online version of this paper).

Characterization of AC-AlCe composites

Scanning electron microscopy (SEM) along with energy dispersive spectroscopy (EDS) analysis was carried out for the AC-AlCe composite after and before F^- sorption. A state-of-the-art thermal field emission scanning electron microscope, Hitachi SU1510, accompanied by an EDS analyzer (ARCI, Hyderabad), was used for the imaging process. The operating voltage was 20 kV and the working distance to the surface of the specimen was 14.0–14.5 mm. The magnifications used for imaging were in the range of 3,000× and 10,000×.

Powder X-ray diffraction (XRD) was also carried for unmodified AC and other AC-AlCe composites using a Bruker AXS D8 Advance X-ray diffractometer. The CuK*a* X-rays were generated at 35 mA and 40 kV. Scans were performed over 0 to 90° 2θ range at 0.02° 2θ steps and integrated at the rate of 32.8 s $step^{-1}$.

Fourier transform infrared (FTIR) spectroscopy analysis was carried out for AC, and the composites before and after F^- sorption to verify the possible chemical changes at the surfaces. FTIR spectra were obtained using a JASCO Model FTIR-4200 using a KBr pellet arrangement, in absorbance mode, within the frequency range of 4,000–400 cm^{-1}.

Sorption experiments

Fluoride removal efficiency: effect of different synthesis parameters

To assess F^- removal efficiency, a series of experiments were carried out with different AC-AlCe composites prepared with varying initial pH (2.5 to 5), and Al-Ce concentration (0.05 mol/L to 0.21 mol/L) treated at different temperatures (120 °C and 240 °C). As a first step, the fluoride stock (100 mg L^{-1}) solution was prepared from NaF salt, and it was diluted to 10 mg L^{-1} F^-. The batch experiments were carried out by adding 70 mL of F^- solutions in a series of bottles, where the concentration of the AC-AlCe composites was kept constant at 5 g/L. The pH of each system was measured after 10 min (stabilization time) and adjusted to 6.5 ± 0.3 by adding 0.1 mol/L of HCl or NaOH. The bottles were kept in a rotator at 50 rpm at room temperature (25 °C). The samples were withdrawn from each bottle after 3 h for analysis.

The AC-AlCe composite prepared with initial Al-Ce concentration of 0.05 mol/L (with Al/Ce = 8:1) and pH of 2.5; and treated at 120 °C [denoted as AC-AlCe-5] was the best performing composite, and thus selected as reference adsorbent for further study. The performance of the composite prepared with the same condition but treated at 240°C [denoted as AC-AlCe-9] is in the proximity in performance of the above composite. Thus, the sorption behavior of fluoride by AC-AlCe-9 composite was also assessed. The concentration of Al and Ce in the solution after the sorption test was measured to check the extent of leachate of impregnated metals in the solution.

Sorption kinetic tests

Sorption kinetics was evaluated for two optimal performing composites namely AC-AlCe-5 and AC-AlCe-9. To evaluate the sorption kinetics, 2 g/L of selected AC-AlCe composite was placed in a series of polyethylene bottles and 70 mL of 50 mg/L of the fluoride-containing solution was poured into each of these bottles. The pH of the solution was adjusted to 6.5 ± 0.3. Samples were withdrawn at different time intervals (i.e., 5, 15, 30, 45, 60, 90, 120 and 180 min) from individual bottles for analysis. A few samples were kept for a longer duration (12 h and 24 h) to ensure the following timescale was sufficient to reach near equilibrium.

Equilibrium sorption experiments

Equilibrium sorption experiments were carried out with composites AC-AlCe-5 and AC-AlCe-9. In this experiment, the concentration of the sorbent composites was kept fixed at 2 g/L, whereas the F^- concentration was varied over an

order of magnitude ranging from 5 mg/L to 55 mg/L. A number of solutions containing various F^- concentrations were poured in a series of polyethylene bottles, each containing 0.14 g of composites (with a fixed pH of 6.5 ± 0.3). The bottles were shaken thoroughly with a rotator for 3 h at 25 °C. Before the experiment, it was assured that 3 h were sufficient time to reach near equilibrium concentration for F^- sorption.

Effect of solution pH on fluoride removal

In a series of bottles, 70 mL of 50 mg/L fluoride solutions were prepared with varying pH value ranging from 4.5 to 10. The pH of the solution was adjusted by adding either 0.1 mol/L HCl or 0.1 mol/L NaOH. To each of these bottles, 0.14 g of AC-AlCe-5 composite was added. The samples were withdrawn after 3 h from the start of the experiment for analysis.

All the experiments were carried out in duplicate or triplicate (F^- removal efficiency), and the mean value is presented in the result. During all sample analysis, fluoride concentration was measured following method EPA-340.2, where by total ionic strength adjustable buffer solution was mixed with the samples (1:1 ratio) to maintain desirable pH range. Then, the fluoride concentration of samples was measured using a fluoride-ion selective electrode.

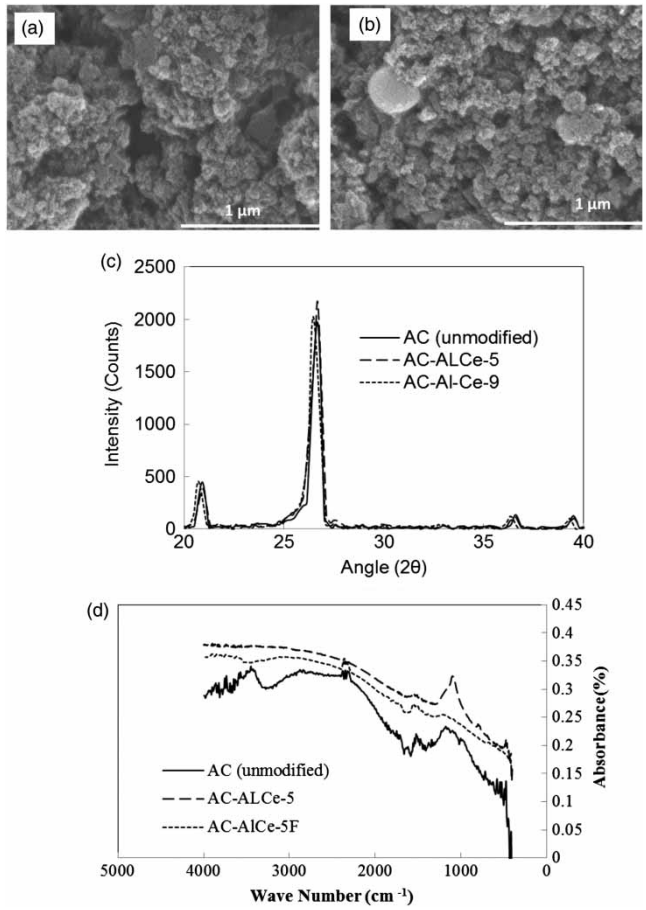

Figure 1 | SEM image of composites (a) AC-AlCe-5 and (b) AC-AlCe-12. (c) XRD spectra of AC and modified AC. (d) FTIR spectra for AC and AC-AlCe-5 composite with and without fluoride sorption.

RESULTS AND DISCUSSION

Characterization

SEM–EDS

SEM images (Figure 1(a) and 1(b) and Supplementary Figure S1a) reveal no significant differences in morphology between unmodified and metal impregnated AC. The presence of nanocrystals of metals could not be detected, even at 10,000 × magnification, which indicates the predominance of amorphous phases of metal. These findings were later corroborated by the results from XRD, which follow a general pattern of flat humps instead of sharp peaks. EDS analysis suggests the presence of silica impurities in the AC (Supplementary Figure S1b). This phenomenon is again confirmed by XRD pattern. The occurrence of impregnated metal (Al-Ce) within the synthesized AC-AlCe composites was confirmed by EDS analysis (Supplementary Figure S1b). (Supplementary Figure S1 is available with the online version of this paper.)

XRD

The XRD pattern of the unmodified AC, as well as double-metal impregnated AC at two different temperatures, are presented in Figure 1(c). Peaks corresponding to quartz were observed, which indicates the presence of silica impurities in the AC. A similar finding was observed in other studies (Raychoudhury *et al.* 2015). However, no visible change was observed in the crystalline structure after impregnation of metal, which suggests probably that the metal present in the microstructure of the composite is in

the amorphous phase (Gu *et al.* 2005; Raychoudhury *et al.* 2015).

FTIR

The FTIR spectra for unmodified AC, AC-AlCe-5 composite, before and after fluoride sorption (AC-AlCe-5F) is presented in Figure 1(d). In the unmodified AC sample, the broad absorbance band at 3,449 cm^{-1} can be assigned to the stretching vibration of the OH group (Abulencia & O'Brien 2012). Another peak can be observed at 1,748 cm^{-1}, which indicates the presence of C = C stretching vibrations (Zhao *et al.* 2013). There is a small peak at 1,508 cm^{-1} due to the C = O stretching vibrations band, and the strong peak at 1,174 cm^{-1} can be assigned to C–O–C stretching vibrations (Abulencia & O'Brien 2012).

After metal impregnation, the peaks observed between 1,200 and 400 cm^{-1} are due to the characteristic vibrations of mixed metals. The strong peak at 1,097 cm^{-1} can be assigned to the bending vibration of hydroxyl groups on metal oxides (Al–OH or Ce-OH) (Liu *et al.* 2010). The strong band at 620 cm^{-1} is the characteristic of metal–oxygen vibration, which is attributed to the Al–O bond (Liu *et al.* 2010). Another small peak at 472 cm^{-1}, indicates the presence of a Ce-O bond (Wang *et al.* 2013). Overall, FTIR analysis indicates the formation of both oxides and hydroxides of both the metals (Al and Ce) on the surface of AC, when treated at 120 °C. Similar observations were made for the composite AC-AlCe-9 (Supplementary Figure S2, available with the online version of this paper), which was treated at 240 °C. However, the chemical shift indicates the greater progress of reaction at a higher temperature.

Effect of synthesis conditions on the performance of the composites

Effect of pH during synthesis

Fluoride removal efficiencies by AC-AlCe composites prepared with varying initial pH ranging from 2.5 to 5 (denoted as AC-AlCe-1 to AC-AlCe-4, Supplementary Table S1) with a total metal concentration of 0.09M are shown in Figure 2(a). The composite AC-AlCe-1, prepared with the lowest pH of 2.5 can remove up to 0.38 ± 0.013 mg of F^- per gram of composite, where the initial concentration of F^- and the composite were kept fixed at 10 mg/L and 5 g/L, respectively. Fluoride removal decreases initially with an increase in synthesis pH to 3 (removal 0.12 ± 0.021 mg/g). However, with further increase in synthesis pH, F^- removal efficiency improved and reaches to 0.21 ± 0.033 mg/g at pH 5. With the increase in pH, the surface charge and hydrophobicity of AC can be altered, which may influence the diffusion of the metal in AC pores. Furthermore, NaOH solution was added to the mixture to raise the pH value of the system. The addition of NaOH leads to the formation of hydroxide precipitates, which can block the micropores of AC and resulted in the reduction of F^- removal efficiency.

The composite AC-AlCe-1 synthesized with a pH value of 2.5 (no pH adjustment) shows the best performance and thus, in the next step the synthesis pH was kept fixed at 2.5.

Effect of morality

Fluoride removal by the AC-AlCe composites, synthesized at a temperature of 120 °C, are improved significantly (0.36–0.43 mg/g) compared to unmodified-AC (0.18 mg/g). With impregnation of a small amount of Al-Ce (0.05 M), the composite AC-AlCe-5 (treated at 120 °C) showed the best performance (0.43 mg/g). At the same hydrolysis temperature, with an increase in metal concentration, the performance of the composite reduces slightly (0.36 mg/g at 0.09 mol/L concentration) and then it gets stabilized (0.35–0.36 mg/g) within Al-Ce concentration range of 0.09 mol/L to 0. 21 mol/L (Supplementary Table S1 and Figure 2(b)). The composite AC-AlCe-9 that contains only 0.05 mol/L of metal and treated at 240 °C can adsorb up to 0.4 mg of F^-/g of composite. Fluoride sorption capacity decreases steadily with the increase in total Al-Ce concentration ranging from 0.09 mol/L to 0.21 mol/L when treated at 240 °C (Figure 2(b)). Similar observation was made for arsenic adsorption. Few studies showed that arsenic removal efficiency by iron impregnated AC reduced with an increase in impregnated iron content in the composite (Hristovski *et al.* 2009; Raychoudhury *et al.* 2015). A recent study by Raychoudhury *et al.* (2015) has demonstrated that impregnation of excess iron in the AC reduces the SSA of the composite due to pore blocking. Pore-blocking eventually reduces the arsenic removal efficiency. Thus, in this

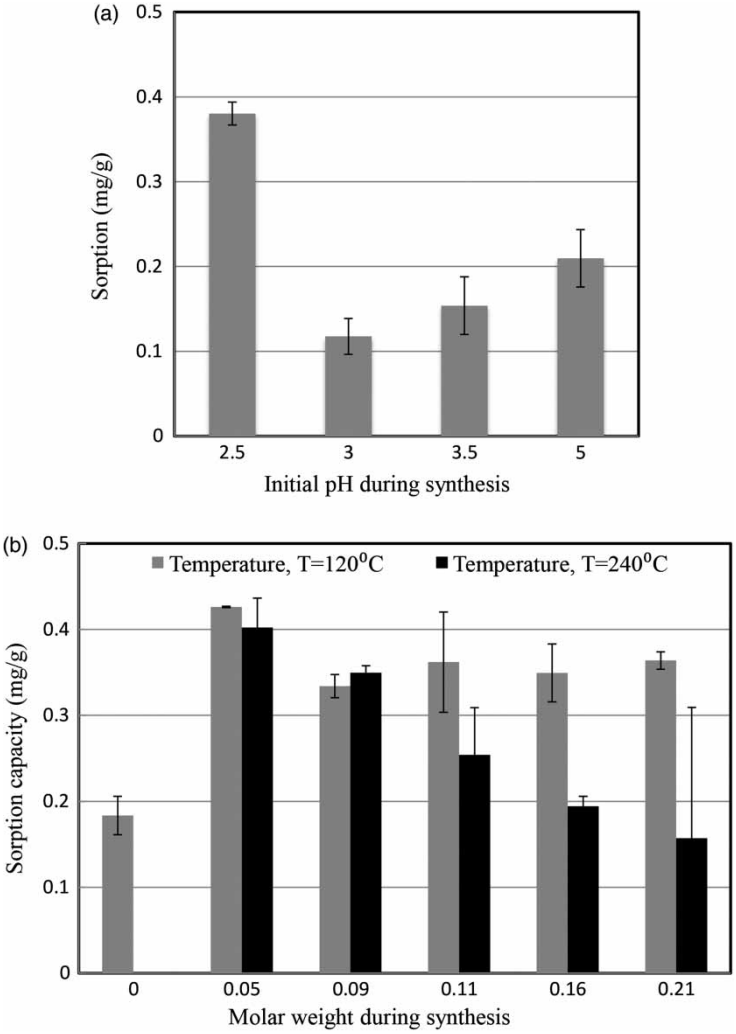

Figure 2 | Fluoride removal efficiencies by different AC-AlCe composites synthesized under (a) varying initial pH with a constant metal concentration of 0.05 mol/L and (b) varying metal concentration and temperature without adjusting initial pH. The concentration of F^- was 10 mg/L and the initial pH of F^- containing water was 6.5 ± 0.3.

study, it could be inferred that decrease in F^- removal with an increase in metal concentration (especially at higher concentration) can probably be attributed to pore blocking.

Overall, the composites AC-AlCe-5 and AC-AlCe-9, prepared with lowest initial Al-Ce concentration (0.05 mol/L) under lowest pH (2.5), showed the best performances with fluoride removal capacities of 0.43 mg/g and 0.40 mg/g, respectively. The concentration of metals was measured in the treated solution. Cerium concentration was found below the detection limit. However, Al concentration in the solution was significantly high (around 1 mg/L). Leachate of Al in considerable quantity is probably reducing the performance of the composite. However, given the performance of all the composites, AC-AlCe-5 and AC-AlCe-9 are selected as the reference adsorbent and considered for further study.

Sorption behavior

Sorption kinetics

Sorption of F^- by both AC-AlCe-5 and AC-AlCe-9 composite with respect to time were observed over a period of 180 min as presented in Figure 3(a). The experimental data were compared with the pseudo-first-order and pseudo-second-order kinetics model (equations in Table 1). Model

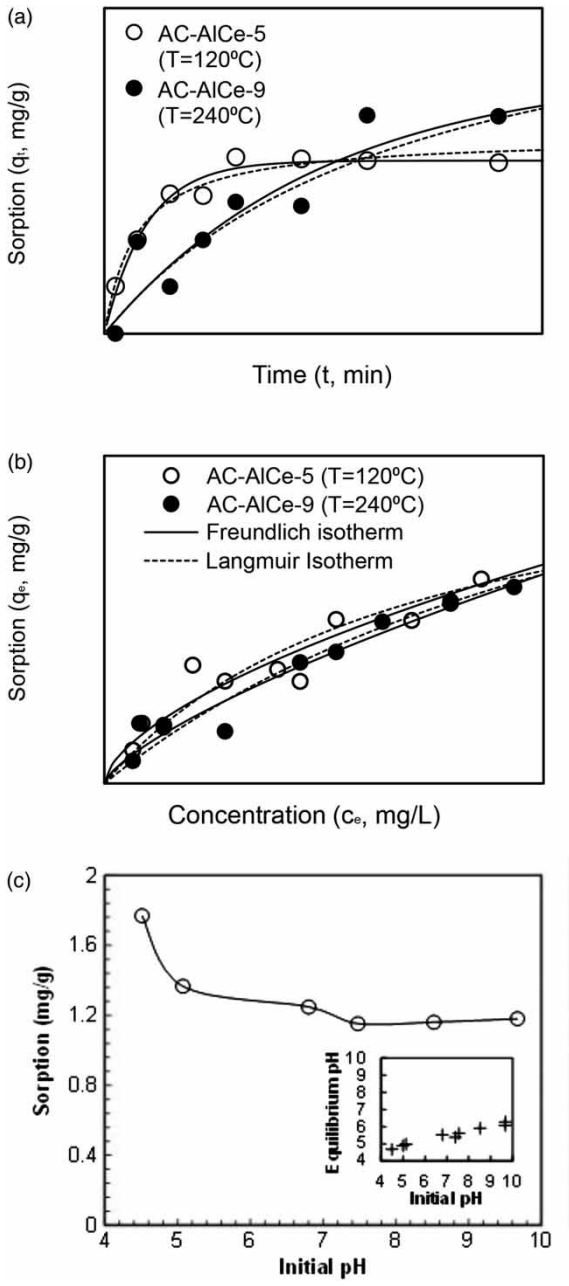

Figure 3 | (a) Sorption kinetics and (b) isotherm of fluoride by the selected AC-AlCe composites at pH of 6.5 ± 0.3. The composite content was 2 g/L for all experiments. In the kinetics test, fluoride concentration was kept fixed at 50 mg/L and for the isotherm test, the concentration of fluoride was varying. (c) Effect of pH on fluoride removal by AC-AlCe-5 composite. The concentration of fluoride and the composite was fixed at 50 mg/L and 2 g/L, respectively.

parameters were estimated by least square error minimization between the model simulation and the experimental data. The estimated parameters, the coefficient of determination (r^2) and the mean least square of error ($\sum\varepsilon$) values for the different model are presented in Table 1.

Fluoride sorption rate by AC-AlCe-5 composite is explained better by pseudo-first-order kinetics (r^2_{ft}: 0.958) compared to the pseudo-second-order kinetics (r^2_{ft}: 0.946) model. Greater extent of physisorption and leaching of fluoride along with aluminum might have resulted in a better fit to the pseudo-first-order kinetics model for AC-AlCe-5. Wu *et al.* (2007) have also observed a better fit of the pseudo-first-order kinetics model to the fluoride sorption kinetics data when trimetallic Al-Ce-Fe was used as an adsorbent. For AC-AlCe-9 composite, the values of r^2 for the pseudo-first-order (r^2_{ft}: 0.856) and second-order kinetics (r^2_{ft}: 0.858) model fits are in very close proximity. However, the pseudo-second-order kinetics model explains the data slightly better than the pseudo-first-order kinetics model. At high synthesis temperature, the extent of chemisorption might be greater for AC-AlCe-9 composite, resulting in a slightly better fit to the pseudo-second-order model. In some other studies, the sorption kinetics of F^- by different metal-based adsorbent were better explained by pseudo-second-order kinetics model (Dou *et al.* 2011; He *et al.* 2014; Zhang *et al.* 2014; Yu *et al.* 2015). Considering, pseudo-first-order sorption kinetics, the rate of fluoride sorption by AC-AlCe-5 composite (0.057 1/min) is more than 5 times faster than that of AC-AlCe-9 composite (0.01 1/min). The rate of fluoride sorption by Al-Ce-Fe based metal (Wu *et al.* 2007) and Zr-embedded PSF (He *et al.* 2014) are reported as 0.0029 1/min and 0.003 1/min, respectively. The rates of F^- sorption by the above-mentioned composites are one order of magnitude less compared to that of our study (0.01–0.057 1/min).

In general, sorption kinetics is controlled by different processes, such as (i) solute mass transfer from the bulk solution to the thin film, (ii) diffusion of solute through film boundary layer, and (iii) sorption/adsorption of solute at the solid surface (Ho & McKay 2000; Argun *et al.* 2007). The sorption kinetics data were compared with the Weber–Morris model (described in Supplementary Material, available with the online version of this paper) to get insight into the sorption process. Multiple linear relationships between adsorbed mass (q_t) and root square of time ($t^{1/2}$) were obtained with r^2 values of 0.95 and 0.99 for AC AlCe-5 (Supplementary Figure S3, available with the

Table 1 | Sorption kinetics and equilibrium isotherm results for the composites AC-AlCe-5 and AC-AlCe-9

	Pseudo-first-order $q_t = q_{e1}(1 - e^{-k_t t})$				Pseudo-second-order $q_t = \frac{k'_t q_{e2}^2 t}{1 + k'_t q_{e2} t}$			
Samples	q_{e1} (mg/g)	k_t (1/min)	r_{ft}^2	$\sum\varepsilon_{ft}$	q_{e2} (mg/g)	k'_t (g/mg/min)	r_{st}^2	$\sum\varepsilon_{st}$
AC-AlCe-5 (T = 120 °C)	1.06	0.052	0.958	0.02	1.21	0.057	0.946	0.03
AC-AlCe-9 (T = 240 °C)	1.62	0.01	0.856	0.22	2.36	0.003	0.858	0.21

	Freundlich model $q_e = k_f c_e^{1/n}$				Langmuir model $q_e = \frac{q_{max} k_l c_e}{1 + k_l c_e}$			
Samples	$k_f \left(\frac{mg/g}{(mg/l)^{1/n}}\right)$	$1/n$	r_f^2	$\sum\varepsilon_f$	q_{max} (mg/g)	k_l (l/mg)	r_l^2	$\sum\varepsilon_l$
AC-AlCe-5 (T = 120 °C)	0.11	0.61	0.912	0.14	**2.20**	0.024	0.878	0.18
AC-AlCe-9 (T = 240 °C)	0.067	0.72	0.937	0.07	**3.05**	0.012	0.929	0.08

q_t: adsorbed mass at time t, q_{e1} & q_{e2}: are the fitted value of adsorbed mass at equilibrium for pseudo-first order and second-order kinetics model, respectively. k_t and k'_t pseudo-first and second order rate constant, respectively. c_e: equilibrium concentration; q_e: adsorbed mass at equilibrium, k_f, and $1/n$: Freundlich sorption constants, q_{max}: maximum sorption capacity, k_l: Langmuir sorption constant. r_{ft}^2, r_{st}^2, r_f^2 and r_l^2, are the r^2 values for pseudo first order, second order kinetics, Freundlich and Langmuir isotherm models, respectively.

online version of this paper). A linear curve can fit the kinetics data for AC-AlCe-9 composite moderately well ($r^2 = 0.70$). In both cases the linear curve is not passing through the origin, suggesting the rate limiting factor is complex in nature. Most likely, in addition to intra-particular diffusion, mass transfer from bulk solution and boundary layer diffusion are also playing important roles in limiting the sorption rate (Argun *et al.* 2007; Dou *et al.* 2011). A similar phenomenon was suggested during sorption of heavy metal when adsorbed in the granular material (Argun *et al.* 2007; Raychoudhury *et al.* 2015). The intra-particle diffusion rate is faster for AC-AlCe-5 (0.135 mg/g/min$^{0.5}$) as compared to AC-AlCe-9 (k''_t=0.114 mg/g/min$^{0.5}$), which probably results in a faster rate of sorption for the former (0.057 1/min) compared to the later (0.01 1/min) composite.

Equilibrium sorption isotherm

Equilibrium sorption experiments were carried out to evaluate the liquid phase–solid phase partitioning of fluoride, using AC-AlCe-5 and AC-AlCe-9 composites as the sorbent. The results are shown in Figure 3(b). Freundlich and Langmuir isotherm models were fitted to the data following nonlinear least square error minimization approach. Comparison of r^2 and $\sum\varepsilon$ values, given in Table 1, suggests fluoride sorption at equilibrium by AC-AlCe-5 composites can be explained much better by Freundlich isotherm model (r_f^2: 0.912) compared to Langmuir isotherm model (r_l^2: 0.878). Fluoride sorption by the composite AC-AlCe-9 is also explained slightly better by Freundlich (r_f^2: 0.937) isotherm model compared to Langmuir isotherm model (r_l^2: 0.929). Some other studies have similarly found that Freundlich isotherm model is a better fit to the fluoride sorption trend when adsorbed by manganese–zirconium composite (Tomar *et al.* 2013), and granular zirconium–iron oxide based composite (Dou *et al.* 2011). In this study, sorption by both the composites is explained better by the Freundlich model, which suggests the composite might have a heterogeneous surface with non-uniform distribution of active adsorption sites. Furthermore, monolayer sorption is probably not governing fluoride removal within the concentration range

(5–50 mg/l) used in this study. The value of the Freundlich constant ($1/n$) for AC-AlCe-5 composite (0.61) is less than 1 and even smaller than that of AC-AlCe-9 composite (0.72), indicating favorable sorption sites at the low fluoride concentration.

Estimation of Langmuir isotherm model parameters suggests that the maximum F^- sorption capacities by the AC-AlCe-5 and AC-AlCe-9 composites are 2.20 mg/g and 3.05 mg/g, respectively. Fluoride sorption capacity, estimated in this study is slightly higher than the range reported in other studies. For example, maximum F^- sorption capacity by lanthanum–aluminum loaded scoria was estimated as 1.25 mg/g (Zhang *et al.* 2014). Alginates iron–zirconium composite can adsorb up to 1.8 mg F/g of adsorbent (Swain *et al.* 2013). Maximum fluoride adsorption by zirconium-loaded AC is 1.83 mg/g. However, impregnation of ZrO_x resulted in an increase in fluoride sorption up to 7.39 mg/g (Velazquez-Jimenez *et al.* 2014). Fluoride sorption capacities vary within a wide range for different metal or LDH based adsorbents. For example, Tomar *et al.* (2013) have reported a maximum fluoride removal capacity of 3.05 mg F^-/g of the manganese-zirconium bimetallic composite. Where, tri-metallic Al-Fe-Ce can remove up to 178 mg F^-/g metal adsorbent (Wu *et al.* 2007). Fluoride sorption capacity by Al-Ce LDH was reported as high as 68 mg/g LDH (Liu *et al.* 2010). It is important to note that in this study, only a small amount of metals are impregnated in the pore spaces of AC. Considering the percentage of impregnated metal estimated from ICP-AES analysis (2.7% in AC-AlCe-5 and 2.6% in AC-AlCe-9), the maximum fluoride sorption capacities by AC-AlCe-5 and AC-AlCe-9 composites are 84 mg F/g Al-Ce and 117 mg F/g Al-Ce, respectively. The maximum F^- sorption capacities by the AC-AlCe composites are reasonably high and comparable to bimetal-based adsorbent reported in other studies.

To get insight into the fluoride removal mechanism at equilibrium, FTIR analysis was conducted after fluoride sorption (Figure 1(d)). The bands at 3,449 cm^{-1} shifted to 3,561 cm^{-1}, indicating the interaction of fluoride with the hydroxyl groups in the sorbent (Liu *et al.* 2010). Moreover, new peaks were observed at 1,541 cm^{-1} and 1,374 cm^{-1} in the spectrum of the fluoride-sorbed composite, which indicate the presence of the Ce–F and Al–F bonds formed after F^- adsorption (Liu *et al.* 2010). This result suggests a chemical interaction of fluoride with the Al and Ce oxides and hydroxides present at the surface of the AC. A similar observation was made for the composite AC-AlCe-9 (Supplementary Figure S2). However, the chemical shift confirmed the greater progress of the chemisorption of the fluoride at a higher temperature.

Effect of pH on fluoride removal

The effects of pH, within a range of 4.5 ± 0.1 to 9.7 ± 0.1, on fluoride removal by the composite AC-AlCe-5, were presented in Figure 3(c). Sorption of F^- at a pH value of 4.5 ± 0.1 was observed to be 1.77 ± 0.28 mg/g and with an increase in pH value to 5, it reduces to 1.35 ± 0.27 mg/g. With further increase in pH the sorption capacity of F^- decreases slightly, and at a pH value of 9.7, the F^- removal capacity by the composite reached 1.18 ± 0.082 mg/g. In brief, over a wide range of pH (5 to 10), the effect of pH on F^- removal is negligible. This phenomenon can make this composite suitable for treating water or wastewater from different sources having a wide range of pH. The maximum F^- removal efficiency within a pH range of 4 to 5 was observed in a few other studies by different metal-based composite (Chai *et al.* 2013; He *et al.* 2014). AC-AlCe-5 composite has a typical characteristic where, with a wide range of initial pH (4.5–9.7), the equilibrium (or final) pH of the treated water was restricted within a narrow range (4.2 to 6.3, Figure 3(c)). This characteristic of the composite can make it suitable for treating drinking water from various sources.

CONCLUSION

Impregnation of a small amount of suitable metal can enhance the fluoride removal efficiency significantly, compared to unmodified granular activated carbon. Fluoride sorption rate by the composite is reasonably fast (3.6 /h). Sorption of the composite follows the Freundlich isotherm model, with $1/n$ value less than 1. This suggests, even at low fluoride concentration, which is more relevant for natural groundwater conditions, that removal of fluoride from the water will be efficient. FTIR analysis confirms strong chemical bonding between fluoride and oxides of Al and Ce metal impregnated within the pores spaces of AC. Furthermore, fluoride removal was observed to be reasonably consistent over a wide range of pH (5 to 10). This sorption

behavior indicates that the composite has the potential for treating water and wastewater from different sources. Leachate of cerium in the solution is insignificant, which makes cerium suitable for use as an adsorbent. However, a considerable quantity of Al is released into the water, which reduces the performance of the composite. Thus, there is future scope to synthesize novel composite with limited use of Al.

REFERENCES

Abulencia, J. P. & O'Brien, S. 2012 A sustainable water purification solution for rural communities. *International Journal of Environmental Pollution and Remediation* **1** (1), 75–81.

Argun, M. E., Dursun, S., Ozdemir, C. & Karatas, M. 2007 Heavy metal adsorption by modified oak sawdust: thermodynamics and kinetics. *Journal of Hazardous Materials* **141** (1), 77–85.

Bhatnagar, A., Kumar, E. & Sillanp, M. 2011 Fluoride removal from water by adsorption – a review. *Chemical Engineering Journal* **171** (3), 811–840.

Chai, L. Y., Wang, Y. Y., Zhao, N., Yang, W. C. & You, X. Y. 2013 Sulfate-doped Fe_3O_4/Al_2O_3 nanoparticles as a novel adsorbent for fluoride removal from drinking water. *Water Research* **47** (12), 4040–4049.

Chang, Q., Lin, W. & Ying, W.-C. 2010 Preparation of iron-impregnated granular activated carbon for arsenic removal from drinking water. *Journal of Hazardous Materials* **184** (1–3), 515–522.

Choi, H., Al-Abed, S. R., Agarwal, S. & Dionysiou, D. D. 2008 Synthesis of reactive nano-Fe/Pd bimetallic system-impregnated activated carbon for the simultaneous adsorption and dechlorination of PCBs. *Chemistry of Materials* **20** (11), 3649–3655.

Dou, X., Mohan, D., Pittman Jr, C. U. & Yang, S. 2011 Remediating fluoride from water using hydrous zirconium oxide. *Chemical Engineering Journal* **198–199**, 236–245.

Gu, Z. M., Fang, J. & Deng, B. L. 2005 Preparation and evaluation of GAC-based iron-containing adsorbents for arsenic removal. *Environmental Science & Technology* **39** (10), 3833–3843.

He, J., Siah, T.-S. & Paul Chen, J. 2014 Performance of an optimized Zr-based nanoparticle-embedded PSF blend hollow fiber membrane in treatment of fluoride contaminated water. *Water Research* **56**, 88–97.

Ho, Y. S. & McKay, G. 2000 The kinetics of sorption of divalent metal ions onto sphagnum moss peat. *Water Research* **34** (3), 735–742.

Hristovski, K. D., Westerhoff, P. K., Moller, T. & Sylvester, P. 2009 Effect of synthesis conditions on nano-iron (hydr)oxide impregnated granulated activated carbon. *Chemical Engineering Journal* **146** (2), 237–243.

Liu, H., Deng, S. B., Li, Z. J., Yu, G. & Huang, J. 2010 Preparation of Al-Ce hybrid adsorbent and its application for defluoridation of drinking water. *Journal of Hazardous Materials* **179** (1–3), 424–430.

Miretzky, P. & Cirelli, A. F. 2011 Fluoride removal from water by chitosan derivatives and composites: a review. *Journal of Fluorine Chemistry* **132** (4), 231–240.

Mohapatra, M., Anand, S., Mishra, B. K., Giles, D. E. & Singh, P. 2009 Review of fluoride removal from drinking water. *Journal of Environmental Management* **91** (1), 67–77.

Raychoudhury, T. & Scheytt, T. 2013 Potential of zerovalent iron nanoparticles for remediation of environmental organic contaminants in water: a review. *Water Science and Technology* **68** (7), 1425–1439.

Raychoudhury, T., Schiperski, F. & Scheytt, T. 2015 Distribution of iron in activated carbon composites: assessment of arsenic removal behavior. *Water Science and Technology: Water Supply* **15** (5), 990–998.

Swain, S. K., Patnaik, T., Patnaik, P. C., Jha, U. & Dey, R. K. 2013 Development of new alginate entrapped Fe(III)-Zr (IV) binary mixed oxide for removal of fluoride from water bodies. *Chemical Engineering Journal* **215–216**, 763–771.

Tomar, V., Prasad, S. & Kumar, D. 2013 Adsorptive removal of fluoride from water samples using Zr-Mn composite material. *Microchemical Journal* **111**, 116–124.

Velazquez-Jimenez, L. H., Hurt, R. H., Matos, J. & Rangel-Mendez, J. R. 2014 Zirconium-carbon hybrid sorbent for removal of fluoride from water: oxalic acid mediated Zr(IV) assembly and adsorption mechanism. *Environmental Science & Technology* **48** (2), 1166–1174.

Wang, J., Xu, W., Chen, L., Jia, Y., Wang, L., Huang, X.-J. & Liu, J. 2013 Excellent fluoride removal performance by CeO_2-ZrO_2 nanocages in water environment. *Chemical Engineering Journal* **231**, 198–205.

WHO 2006 *Guidelines for Drinking-water Quality*. World Health Organization, Geneva, p. 595.

Wu, X., Zhang, Y., Dou, X., Zhao, B. & Yang, M. 2007 Fluoride adsorption on an Fe-Al-Ce trimetal hydrous oxide: characterization of adsorption sites and adsorbed fluorine complex species. *Chemical Engineering Journal* **223**, 364–370.

Yu, Y., Wang, C., Guo, X. J. & Chen, P. 2015 Modification of carbon derived from *Sargassum* sp. by lanthanum for enhanced adsorption of fluoride. *Journal of Colloid and Interface Science* **441**, 113–120.

Zhang, S., Lu, Y., Lin, X., Su, X. & Zhang, Y. 2014 Removal of fluoride from groundwater by adsorption onto La(III)- Al(III) loaded scoria adsorbent. *Applied Surface Science* **303**, 1–5.

Zhao, H., Wang, F., Ning, Y., Zhao, B., Yin, F., Lai, Y., Zheng, J., Hu, X., Fan, T., Tang, J., Zhang, D. & Hu, K. 2013 Green 'planting' nanostructured single crystal silver. *Scientific Reports* **3**, 1511.

First received 18 March 2016; accepted in revised form 17 June 2016. Available online 11 July 2016